

Extreme Neutron Rich Sector of the Nuclear Chart: New Horizons!

K. A. Gridnev^a, V. N. Tarasov^b, D. K. Gridnev^{a,c},
D. V. Tarasov^b, X. Viñas^d and Walter Greiner^c

^a*Department of Physics, St. Petersburg State University, 1 Ulyanovskaya st., St. Petersburg 198504, Russia*

^b*NSC, Kharkov Institute of Physics and Technology, 1 Akademicheskaya st., 61108 Kharkov, Ukraine*

^c*FIAS, Frankfurt University, 1 Ruth-Moufang-Str., Frankfurt am Main 60438, Germany*

^d*Facultat de Física, Universitat de Barcelona, 1 Martí i Franquès, Barcelona E-08028, Spain*

Abstract

Using Hartree-Fock + BCS approach we analyze the behavior of the neutron drip line and predict the appearance of stability peninsulas. The conditions and mechanism for appearance of such peninsulas are analyzed and the properties of newly predicted stable isotopes are investigated.

Keywords: *Hartree-Fock method; BCS; stability; neutron drip line*

One of the fundamental questions in nuclear physics is what combinations of neutrons and protons can build up a stable nucleus. The nuclear landscape called nuclear chart is shown in Figs. 1, 2, 3. A large number of stable isotopes are still nuclear “terra incognita”. Moving away from stable nuclei by adding either protons or neutrons, one finally reaches the particle drip lines where the nuclear binding ends. Nuclei beyond the drip lines are unbound with respect to nucleon emission; that is, for those systems the strong interaction is unable to bind up the constituent nucleons as one nucleus.

The main objective of my talk is to discuss some interesting new qualitative features of the neutron drip line that were predicted in [1, 2, 3, 4], namely, the formation of stability peninsulas. A relatively recent experiment [5] revealed new squares on the nuclear chart, which correspond to stable isotopes ⁴⁰Mg and ⁴²Al. Fig. 1 shows also comparison with existing theoretical predictions. Interestingly, the Nature chooses the most optimistic theoretical scenario regarding stability of isotopes at the drip line. So far the experiment is not capable to detect the entire neutron drip line and, as can be seen in Fig. 2, it is, probably, very far from that. It is, of course, important to foresee the experimental setup that would be able to confirm or invalidate present theoretical predictions.

In our discussion we shall focus on even-even nuclei. A reliable microscopic description of nuclei is obtained with the so-called effective forces between nucleons called Skyrme forces. Their use has become popular since the seminal papers of Vautherin and Brink [6], where these forces were successfully used for systematic description of spherical and deformed nuclei. These forces generally predict very well deformations, sizes, nuclear densities, nucleon separation energies, etc. Their advantage is a relatively small number of parameters and delta-functions in the interaction terms, which facilitate the calculation of integrals considerably.

Let us write out an explicit expression of the Skyrme interaction:

$$V_{ij} = t_0(1 + x_0 P_\sigma)\delta(\mathbf{r}) + \frac{1}{2}t_1(1 + x_1 P_\sigma)[\mathbf{k}'^2\delta(\mathbf{r}) + \delta(\mathbf{r})\mathbf{k}^2] + t_2(1 + x_2 P_\sigma)\mathbf{k}'\delta(\mathbf{r})\mathbf{k} + \frac{1}{6}t_3(1 + x_3 P_\sigma)\rho^\alpha(\mathbf{R})\delta(\mathbf{r}) + iW_0[\mathbf{k}' \times \delta(\mathbf{r})\mathbf{k}](\sigma_i + \sigma_j), \quad (1)$$

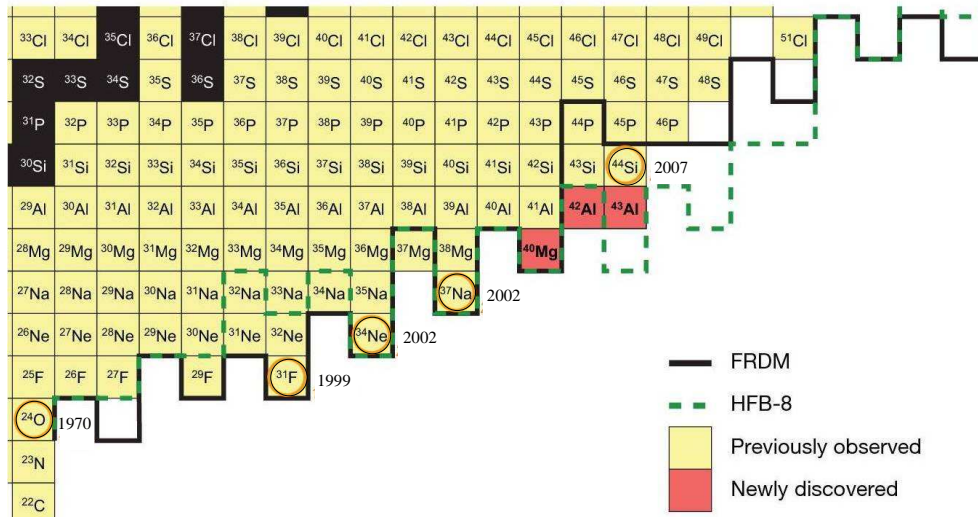


Figure 1: Fragment of the nuclear chart. The proton number increases vertically and the neutron number horizontally. Light squares denote previously observed nuclei. The neutron drip lines predicted by the FRDM and HFB-8 models are shown by the solid and dashed lines, respectively. Recently observed drip-line nuclei are indicated by circles with their year of discovery. The latest discovery also includes ^{40}Mg , ^{42}Al and ^{43}Al which are highlighted with dark fill, see [5].

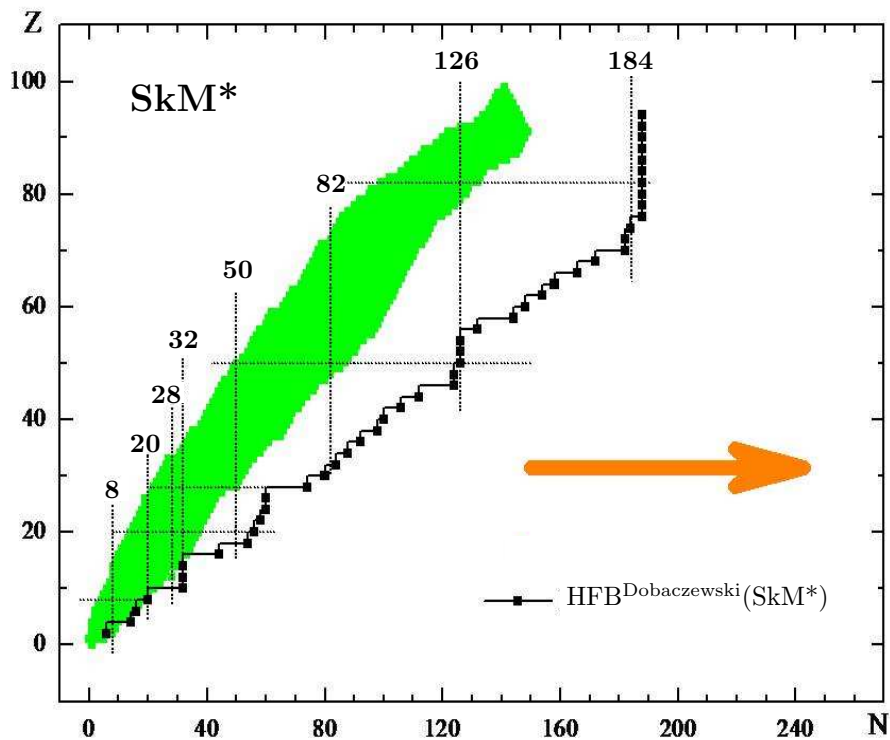


Figure 2: Nuclear chart. Filled area shows experimentally observed nuclei. Black squares correspond to the neutron drip line calculated with the Hartree–Fock–Bogoliubov method [7–8]. The arrow indicates typical direction of the calculations, when one tries to detect the drip line, namely, one increases the neutron number until the saturation point is reached.

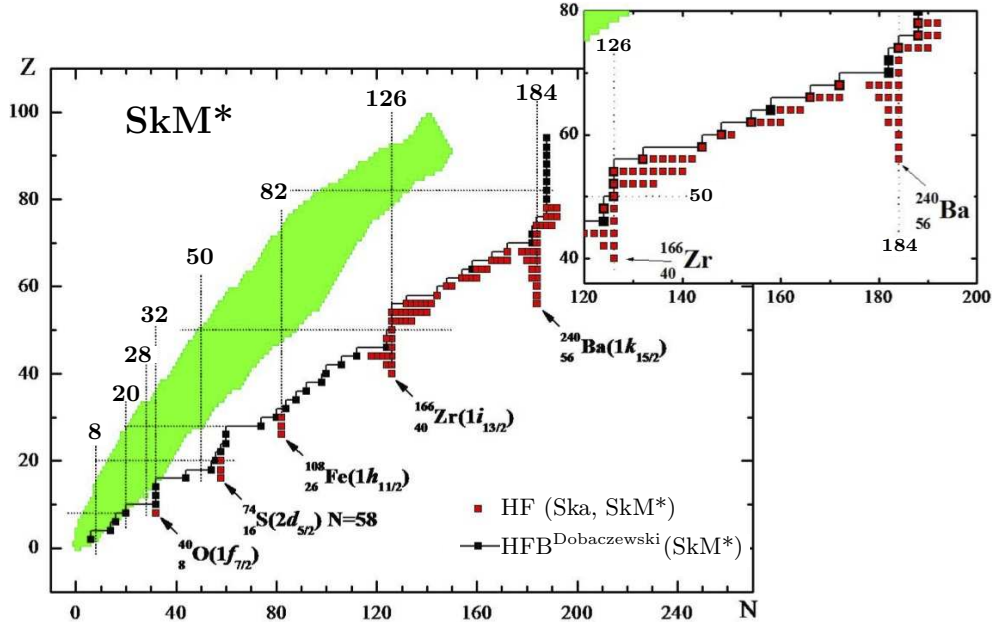


Figure 3: Formation of peninsulas at the neutron drip line. Black squares indicate the drip line obtained within HFB approach using SkM* forces. Filled area shows experimentally known nuclei. Grey squares are nuclei that are predicted stable against one neutron emission in our calculations using Ska and SkM* forces. One can see formation of peninsulas at “magic” numbers and “quenched magic” numbers (see text for details).

where $\mathbf{r} = \mathbf{r}_i - \mathbf{r}_j$, $\mathbf{R} = (\mathbf{r}_i + \mathbf{r}_j)/2$, $\mathbf{k} = -i(\vec{\nabla}_i - \vec{\nabla}_j)/2$, $\mathbf{k}' = -i(\vec{\nabla}_i - \vec{\nabla}_j)/2$, $P_\sigma = (1 + \sigma_i \sigma_j)/2$.

One can see that the force is density dependent. The parameters entering the expression are usually fixed so as to reproduce various bulk nuclear properties as well as selected properties of certain doubly magic nuclei. Some Skyrme forces are presented in Table 1. There is no unique set of parameters and this leads to various versions of the Skyrme force, each of which has its advantages and disadvantages.

After fixing the parameters, the Skyrme forces are used as ingredient in Hartree–Fock calculations, where the ground state wave function is written in the form of a Slater determinant. One also has to introduce a pairing force, which in our case is

Table 1: Parameters of Skyrme forces.

Force	t_0	t_1	t_2	t_3	W_0
	MeV fm ³	MeV fm ⁵	MeV fm ⁵	MeV fm ^{3+3α}	MeV fm ⁵
Sly4	-2488.91	486.82	-546.39	13777.0	123.0
Ska	-1602.78	570.88	-67.70	8000.0	125.0
SkM*	-2645.00	410.00	-135.00	15595.0	130.0

Force	x_0	x_1	x_2	x_3	α
Sly4	0.834	-0.344	-1.0	1.354	1/6
Ska	-0.020	0.0	0.0	-0.286	1/3
SkM*	0.090	0.0	0.0	0.0	1/6

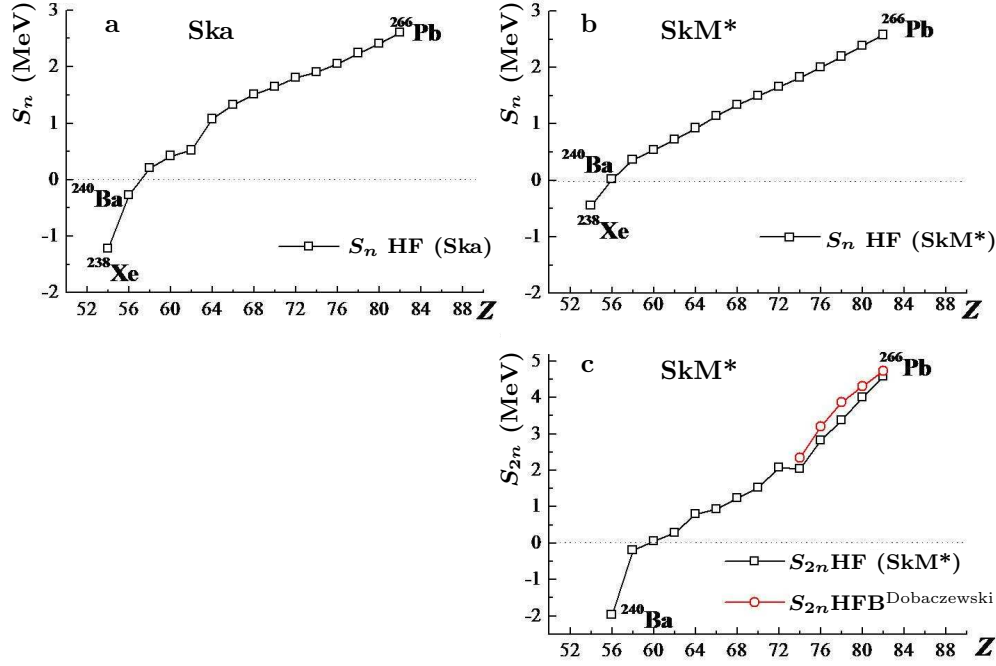


Figure 4: One and two neutron separation energies for the isotones with $N=184$ calculated with Ska, SkM* forces. Circles correspond to HFB calculations [7, 8]. The last element, which is stable against one and two neutrons emission, is ^{244}Nd .

treated in the BCS framework with a pairing constant. We use two procedures to solve Hartree–Fock equations. In the DHF method, which is always used in the case of deformed nuclei, the Hartree–Fock equations are solved using basis functions of the deformed harmonic oscillator. Since we focus our attention on the neutron drip line, one encounters wave functions which correspond to small neutron separation energies, and therefore are very spatially extended. Clearly, one needs basis functions that match such exotic behavior. This is done by adjusting the parameters of the harmonic oscillator on each iteration step. The parameters of the oscillator are chosen in order to minimize the resulting total energy. This helpful procedure of readjusting basis functions reduces substantially the required basis dimension as well as the required number of iterations. In the case of nuclei with spherical symmetry we also employ the SPH procedure, where the equations after reductions due to symmetry are solved on a grid.

In the BCS pairing scheme of DHF calculations, we include only bound one particle states. In spite of ignoring the continuum states this method still provides a good agreement with the HFB (Hartree–Fock–Bogoliubov) calculations [7, 8], see Fig. 4 for comparison. In the BCS scheme of the spherical code, we implement the inclusion of quasibound continuum states which are confined under the centrifugal barrier. To spot such states one introduces a fictitious “wall” forcing the wave functions to vanish beyond it. States remaining localized when the wall is being moved at a large distance, are regarded quasistable and taken into account in the pairing scheme.

The standard theoretical approach in locating the neutron drip line is to take a stable nucleus with a fixed proton charge Z and increase the number of neutrons N until the resulting nucleus would be “overloaded” in the sense that it gets rid of extra neutrons through decay, see Fig. 2. This method, however, implies a simple structure of the drip line, namely, that every line corresponding to a fixed number of protons on the nuclear chart crosses the neutron drip line only once. Yet, it might happen that the drip line has a more complicated structure [1, 2, 3, 4]. In the vicinity of “magic”

numbers or “quenched magic” numbers the following scenario can take place. At some point being filled with neutrons the nucleus loses its stability but then after adding more neutrons the stability is restored. This leads to formation of stability peninsulas on the nuclear chart, see Fig. 3.

The analysis of the phenomenon of stability restoration through adding neutrons has been undertaken in [1, 2, 3, 4]. We have considered long isotope rows of the elements Pb, Zr, Ar, Kr, Rn, Gd, Ba, S, as well as many other elements. Thereby, the phenomenon of stability restoration through adding neutrons was in focus. Having found such new isotopes we also investigated their properties like masses, deformation, root mean square radii, etc.

An important point is also that nuclei forming stability peninsulas are spectrally bound in the sense that there exists a well-defined ground state wave function which minimizes the energy functional for such nuclei. At this point they become well-defined objects and the question about their lifetime is correctly formulated. Even though for some nuclei it may be energetically favorable to get rid of two or more neutrons, a large centrifugal barrier of the last filled levels may serve as an indication that this lifetime would be large. For some nuclei the energetically favorable decay would be into four or more neutrons that enhances the lifetime considerably (such decays were not experimentally observed so far).

In searching for extensions of the neutron drip line limits we proceeded in the standard way adding as many neutrons to the nucleus as possible. Having found an unstable nucleus we did not stop and added more neutrons to see whether the stability can be restored. Gradually, the general picture became clear. One can see in Fig. 3 that stability peninsulas are formed at neutron “magic” numbers or “quenched magic” numbers like in the case of ^{40}O ($N = 32$) or ^{74}S ($N = 58$), which correspond to the filled subshells $1f_{7/2}$ and $2d_{5/2}$ respectively. The stability peninsulas extend vertically along the Z axis in the direction of diminishing Z . Fig. 4 shows how the stability peninsula corresponding to $N = 184$ (a closed shell) extends in Z . This can be seen from one and two neutron separation energies of the isotones. Let us also remark that recent calculations confirm the existence of stability peninsula at $N = 258$, see [9].

In our approach we try different versions of the Skyrme force. Let us stress that just by definition for nuclei at the neutron drip line one expects small one and two neutron separation energies. So it would be rather naive to expect that the drip line calculated with effective forces would exactly match the real one. Even for different forces the difference between separation energies is of order of 0.1 MeV. This is why it is important to check the results with various versions of the Skyrme force. It turns out that the neutron numbers where the stability peninsulas appear, are the same for all forces, only the edges of these peninsulas and the degree to which they are extended depend on the specific version of the force. In view of this striking invariance with respect to the choice of the Skyrme force, we claim that such peninsulas constitute a general qualitative feature of the neutron drip line! Again, let us stress that the nucleon distributions are spherical for nuclei lying on stability peninsulas. This results from the fact that the shells are completely filled at magic numbers. Fig. 5 (top) shows the first isotope ^{40}O that was predicted to form a stability peninsula [1]. It also has a spherically symmetric distribution of nucleons.

The mechanism working behind the formation of stability peninsulas, is usually the same in all cases. When one adds neutrons to an unstable nucleus the totally filled subshell immerses from the continuum to the states with negative energy. For example, in Fig. 5 (bottom) we show how this happens in the case of Radon isotopes. The shell effects are the key to the understanding of these phenomena. Below we list some of the isotopes from the stability peninsulas and the subshells responsible for the stability enhancement:

- $1f_{7/2}$ ^{40}O ;

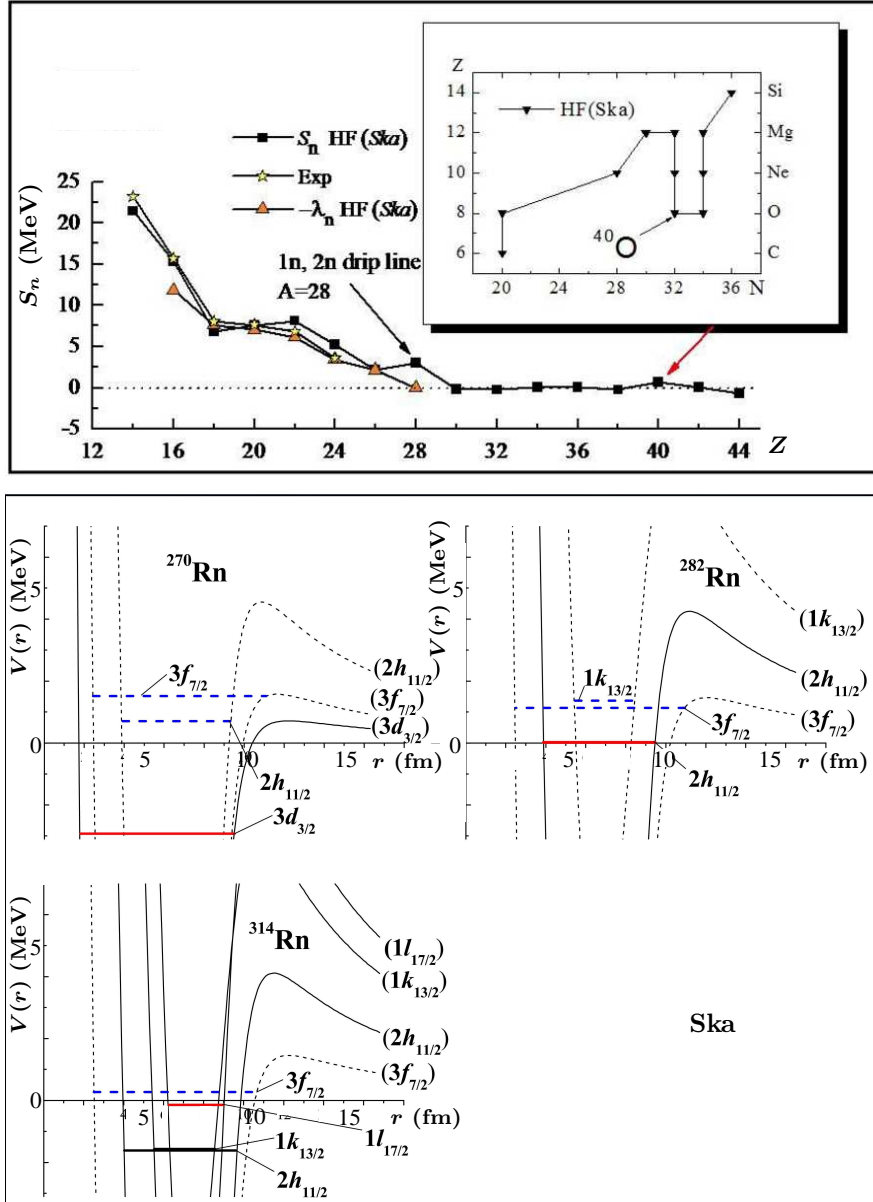


Figure 5: Top: One neutron separation energies of Oxygen isotopes and a fragment of the neutron drip line near ^{40}O . The exotic isotope ^{40}O is stable against one neutron emission and forms a peninsula at the drip line. It has a spherical density distribution. Bottom: the mechanism of stability restoration. In the case of Rn isotopes adding neutrons affects the effective HF potential in such a way that one particle states with high angular momentum are immersed from continuum into the bound spectrum. In the case of magic numbers this leads to stability enhancement. Dashed line show unfilled levels in HF+BCS calculations with Ska forces.

- $2d_{5/2}$ ^{76}Ar , ^{74}S ;
- $1h_{11/2}$ ^{110}Ni , ^{108}Fe ;
- $1i_{13/2}$ ^{174}Cd , ^{172}Pd , ^{170}Ru , ^{168}Mo , ^{166}Zr ;
- $1k_{15/2}$ ^{256}Hf , ^{254}Yb , ^{252}Er , ^{250}Dy , ^{248}Gd , ^{246}Sm , ^{244}Nd , ^{242}Ce , ^{240}Ba .

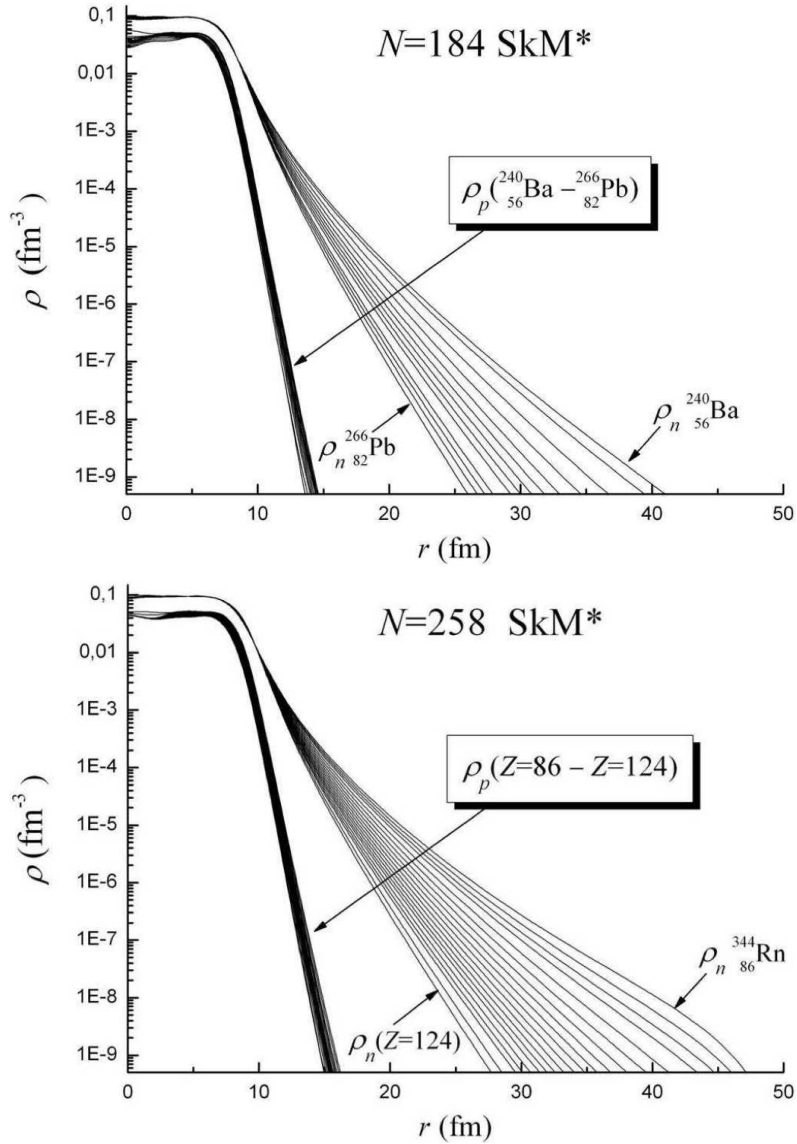


Figure 6: Proton and neutron density distributions for the isotones with $N = 184$ (top) and $N = 258$ (bottom). The calculations are performed with SkM* forces. These are closed shells and the distributions possess spherical symmetry. One can see the enormous spatial extension (halo formation) for a large number of neutrons.

Let us also mention that the wave functions near the drip line produce very spatially extended neutron densities, see Fig. 6. Here one can speak of a large halo formation. To illustrate this we shall compare proton and neutron root mean square radii, which we denote R_p and R_n respectively. For nuclei in the stability valley one has normally $R_n - R_p \simeq 0.1\text{--}0.2$ fm. For ^{40}O we obtain $R_n - R_p \simeq 1.29$ fm and $R_n/R_p \simeq 1.44$. For ^{248}Gd we get $R_n - R_p \simeq 0.77$ fm and $R_n/R_p \simeq 1.14$. For ^{240}Ba we obtain $R_n - R_p \simeq 0.94$ fm and $R_n/R_p \simeq 1.17$.

References

- [1] K. A. Gridnev, D. K. Gridnev, V. G. Kartavenko, V. E. Mitroshin, V. N. Tarasov, D. V. Tarasov and W. Greiner, *Eur. Phys. J. A* **25**, 353 (2005).
- [2] K. A. Gridnev, D. K. Gridnev, V. G. Kartavenko, V. E. Mitroshin, V. N. Tarasov, D. V. Tarasov and W. Greiner, *Phys. Atom. Nucl.* **69**, 3 (2006).
- [3] K. A. Gridnev, V. N. Tarasov, D. V. Tarasov, D. K. Gridnev, V. V. Pilipenko and W. Greiner, *Int. J. Mod. Phys. E* **15**, 673 (2006).
- [4] V. N. Tarasov, D. V. Tarasov, K. A. Gridnev, D. K. Gridnev, V. G. Kartavenko and W. Greiner, *Int. J. Mod. Phys. E* **17**, 1273 (2008).
- [5] T. Baumann *et al.*, *Nature* **449**, 1022 (2007).
- [6] D. Vautherin and D. M. Brink, *Phys. Rev. C* **5**, 626 (1972); *Phys. Rev. C* **7**, 296 (1973).
- [7] M. V. Stoitsov, J. Dobaczewski, P. Ring, and S. Pittel, *Phys. Rev. C* **61**, 034311 (2000); <http://www.fuw.edu.pl/~dobaczew/thodri/thodri.html>.
- [8] M. V. Stoitsov, J. Dobaczewski, W. Nazarewicz, S. Pittel, and D. J. Dean, *Phys. Rev. C* **68**, 054312 (2003).
- [9] V. N. Tarasov, K. A. Gridnev, W. Greiner, S. Schramm, D. K. Gridnev, D. V. Tarasov and X. Viñas, *Bull. Russ. Acad. Sci. Phys.* **76**, 876 (2012).